



Surface Mapping Methods

Y. Le Sant, B. Aupoix, P. Barricau, M.C. Merienne, G. Pailhas, P. Reulet, Y. Touvet

► To cite this version:

Y. Le Sant, B. Aupoix, P. Barricau, M.C. Merienne, G. Pailhas, et al.. Surface Mapping Methods. Aerospace Lab, 2009, 1, p. 1-12. hal-01180577

HAL Id: hal-01180577

<https://hal.science/hal-01180577>

Submitted on 27 Jul 2015

HAL is a multi-disciplinary open access archive for the deposit and dissemination of scientific research documents, whether they are published or not. The documents may come from teaching and research institutions in France or abroad, or from public or private research centers.

L'archive ouverte pluridisciplinaire **HAL**, est destinée au dépôt et à la diffusion de documents scientifiques de niveau recherche, publiés ou non, émanant des établissements d'enseignement et de recherche français ou étrangers, des laboratoires publics ou privés.

Y. Le Sant, B. Aupoix,
P. Barricau, M-C. Mérienne,
G. Pailhas, P. Reulet,
Y. Touvet
(Onera)

E-mail: yves.le_sant@onera.fr

Surface Mapping Methods

The first measurement method used was measuring the forces on the model tested in a wind tunnel. This raised more questions that could only be solved by measuring the pressure on the model's surface. This is still done with pressure taps, but the advent of new optical methods provides a real insight into the flow over the model's surface. Nowadays, all the physical quantities are addressed: pressure, temperature, heat flux, model shape and shear stress.

Introduction

Wind tunnel testing often involves taking physical measurements on the model's surface. These measurements are pressure, temperature and shear stress. There are also derived physical quantities such as heat flux and boundary layer transition. Finally, the surface's shape must be known in order to measure properties, which calls for new measuring methods. All of these variables can be determined using single point sensors or optical methods. The following article mostly concerns the latter type since most of today's research efforts are related to them.

The optical methods are always compared to single point sensor methods and often the end customer has to make a decision taking into account their claimed relative uncertainty. Optical methods undoubtedly have an advantage for temperature measurements and model deformation. In the case of other methods, such as Pressure Sensitive Paint (PSP), the uncertainty of the optical methods is roughly an order of magnitude greater than that of the single point sensors. However, experience has shown that the pressure map offers information of great value that cannot be extracted from a limited number of measurement points. This leads to a rather unexplored field: how can dense experimental results be compared to computational ones? Though this question is obviously also at the heart of flow measurement methods, it is however more challenging for surface mapping methods since the surface pattern of the measured property is of great value because it usually cannot be inferred from single point measurements.

Surface temperature determination is of primordial importance for aerodynamic studies and Infrared thermography, developed over more than 20 years, is the pioneering mapping method. It was an alternative method to thermocouple measurements but is now highly reliable and is even capable of seeing "through the wall", as it will be shown. Temperature Sensitive Paint has been developed at the same time. These two methods are routinely used for many applications.

Surface pressure mapping is also an important issue. Pressure Sensitive Paint or PSP has recently been developed. It consists of measuring the pressure with a luminescent paint. The 90's were the golden age of this method, which is now widespread. It has important

advantages and drawbacks which are explained. In this method, the camera's location in relation to the model must be precisely determined and compensation must also be made for model deformations created by wind loading.

The article then contains the seminal works for a new technique for determining the model's shape called Model Deformation Measurement (MDM). This technique requires unusual precision, which makes it a full method. Finally, shear stress determination, which is the Holy Grail of metrologists, is addressed in final part, which describes how the oil-film method may be the first step in this quest.

Heat flux measurement using infrared thermography

Temperature measurement is probably the most well known surface measurement, due to the widespread use of infrared thermography (*IrT*). Everyone knows that it can be used to "see" where there are hot spots, which is useful in many applications, such as detecting heat sinks and defects in thermal insulation. These kinds of applications are qualitative and quantitative applications that are more connected with R&D fields. There are two kinds of applications for wind tunnel testing. The first one is detecting where the transition from laminar to turbulent is in the boundary layer. Since the heat transfer level is higher in the turbulent area, a temperature discrepancy can be measured through the transition area. The second one is more complicated since it concerns heat flux measurement, which is a derived quantity of the temperature map.

Another technique can also be used for these two kinds of applications. This is TSP, standing for Temperature Sensitive Paint. TSP is very similar to PSP and uses the same devices and nearly the same paints [1]. So when should *IrT* or TSP be used? Both methods have advantages and disadvantages: *IrT* offers an excellent temperature resolution (the best cameras have a resolution of 0.02 K) while the resolution of TSP is usually greater than 0.5 K. On the other hand TSP works in the visible range and therefore has no limitation because of the wide choice of cameras and lenses. This is the really bad point for *IrT* since special windows must be used and the lens choice is dramatically poor.

The paint could be an argument for IrT , but IrT suffers from an extra problem which is emissivity, that is usually too low for metallic parts. As a consequence a special paint is often used with IrR in order to increase the emissivity.

Anyway, IrT is more used than TSP since it is often simpler to apply and does not require any specific post processing to obtain the temperature. But there are some cases in which TSP is used, typically when there is no optical access for IrT .

Measuring heat flux Φ is much more challenging than measuring temperature. The former is deduced from the latter by solving the heat equation [2] which in the 1D case is:

$$\frac{\delta T(x,t)}{\delta t} = \frac{a}{\lambda} \frac{\delta \Phi(x,t)}{\delta x} \quad \text{with} \quad \Phi(x,t) = \lambda \frac{\delta T}{\delta x} \quad (1)$$

This equation shows that Φ depends on the thermal properties (a =diffusivity, λ =conductivity) and on time. That means that the entire temperature histogram must be known. The worst situation is the 3D case where the spatial temperature map must also be taken into account!

However, solving the heat equation is no longer an issue due to dedicated 1D [3] or 3D codes. The output is the heat flux history, which is usually noisy since the heat flux noise is proportional to the first temporal derivative of the temperature noise. A time filter or a space filter based on a small kernel is usually efficient enough to provide smooth results.

As said before, there are two kinds of applications of IrT in wind tunnel testing: boundary layer transition assessment [4] and heat flux measurements in hypersonic facilities. The former is a qualitative application since the aim is simply to visualize the location of the transition area from the laminar part to the turbulent part that enhances the heat flux exchanges between the model surface and the flow. For transonic applications, the temperature step is often lower than 1 K, which is why IrT is a valuable tool since it can be used to visualize temperature changes as low as 0.02 K. Figure 1 shows an old example in a hypersonic facility. The newest cameras (that have improved temperature resolution as well a double image size) have been used in transonic facilities but the images cannot be shown here.

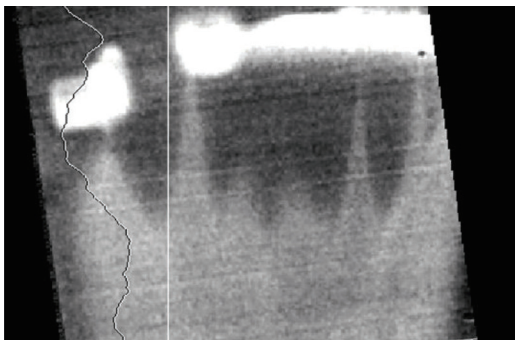


Figure 1 - Visualization of the boundary layer transition in a hypersonic facility. The camera was not well aligned so the image has been mapped on the model grid. This is why there are black parts where the camera did not see anything. The white parts are reflections of the test section's hot spots. The vertical cut shows the temperature profile along a vertical line.

The second application is heat flux measurement in hypersonic facilities [3,5]. The aim is to gather enough quantitative information to design the thermal protection system. As shown in figure 2, the model

is heated quickly by the flow and the three curves have a typical pattern: a parabolic rise followed by a linear rise. The parabolic part at the beginning of the run is the solution of the heat flux equation for a semi-infinite wall while the linear part appears when the thickness of the model surface cannot be neglected.

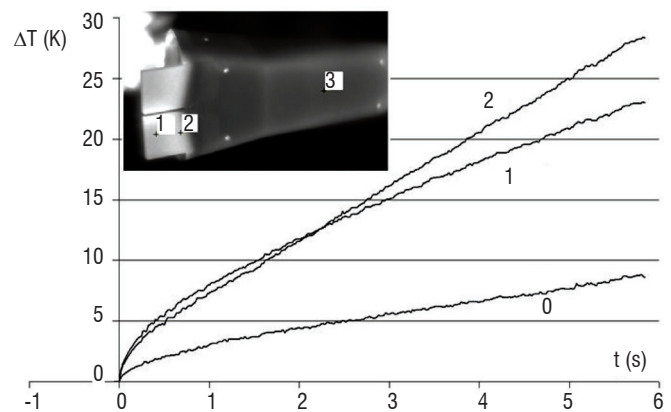


Figure 2 - Temperature history for three points on the PREX model.

Data reduction provides the heat flux history, which is in turn used to provide a unique heat flux value at the beginning of the run, which is presented in figure 3. As expected, the hottest parts are on the flaps while the heat flux level is quite low on the main body and even decreases before the flaps because of flow separation.

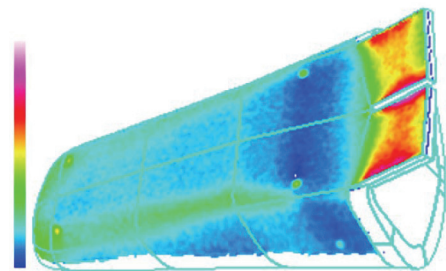


Figure 3 - Heat flux map on the PREX model.

Data reduction is done with a 1D code with some correction to take the 3D lateral conduction into account. However, under severe conditions, this 1D solution is not relevant and a 3D code should be used. This solution is under development and is based on studies carried out in the Onera.

DMAE (Department Aerodynamics and Energetics Modeling) has developed a 3D code that solves the 3D heat flux equation. The applications are to assess the heat flux on a flat plate heated by some heating source like a plasma. Since the heated face cannot be imaged, the opposite face is imaged with an infrared camera. This makes the problem much more complicated since the heat flux level on the heated face has to be deduced from measurements on the non heated face, which is like "seeing through the wall" and is a difficult inverse problem. It is solved by minimizing the functional:

$$E = \int_S \left[T(x) - \int_S f(x,u) \Phi(u) du \right]^2 dx \quad (2)$$

Where S is the model's surface and f is a sensitivity function that returns the effect of the heat flux at the point u on the point x . A regularization method must be used as the Beck's method [6] which assumes that the heat flux is constant for some time duration

Δt , i.e. assessing values at time t by using temperatures at future times. The functional is then:

$$E = \int_{\Delta t} \int_S \left[T(x, t) - \int_S f(x, u, t) \Phi(u) du \right]^2 dx \quad (3)$$

The minimization can be done but often provides noisy results due to the noise on the temperature measurements, which are enhanced. The input data, which is the temperature map, then has to be smoothed using some tool such as the Discrete Cosinus Transform.

The inverse method [7] is used routinely to check the efficiency of heating sources and has even been used in wind tunnel testing [8] as shown in figure 4. The next step is to apply the method to a model with a high 3D feature.

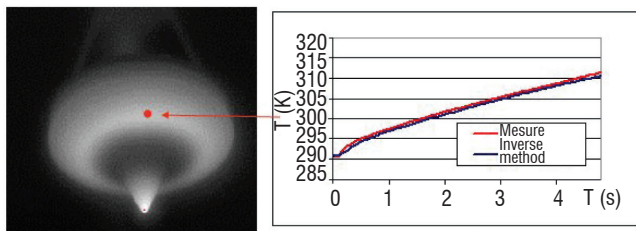


Figure 4 - Infrared measurement on the heated face. A dense thermocouple distribution was used on the non heated face to apply the inverse method. The agreement is fairly good except at the beginning of the run, where the Beck's method fails since the heat flux cannot be considered to be constant.

Box 1- Infrared thermography: uncertainty

Uncertainty for the temperature measurement: 0.03 K for IrT , close to 0.5 K for TSP.
 Uncertainty for the heat flux measurement: since the heat flux is a derived quantity and depends on many quantities, the uncertainty is larger and is often close to 10%.

Surface pressure measurement using Pressure

Sensitive Paint

Until recently, surface pressure measurements in wind tunnel testing were taken solely by pressure taps. Since the 1980's, an optical method has been introduced in order to replace these instruments and is now commonly used in industrial wind tunnels: Pressure Sensitive Paint, or PSP, which is a method generating an image of the pressure surface [9, 10, 11, 12]. The enthusiasm for this technique is prompted by the considerable savings it offers in terms of model instrumentation costs and model construction time, while the wealth of information that can be extracted from the images makes it a preferred investigation tool for complex flows[13]. Moreover, the measured pressure over an entire surface can be integrated to calculate the forces and moments of the complete model, or parts thereof. This article presents the basics of PSP and the way it is used. The PSP principle is relatively simple but requires many precautions if a high level of accuracy is desired.

Pressure sensitivity of luminescence

Practically all existing materials are luminescent in that they emit light when they are excited at a certain wavelength. The emission wavelength is always greater than the excitation wavelength according to Stoke's law. Emission may follow immediately upon excitation, in which case it is called fluorescence, or it may occur later, as in the phenomenon of phosphorescence. The emission intensity and spectrum depend on many parameters[14].

For the molecules used in PSPs, the oxygen captures a part of the decay energy as shown in Figure 5. The molecules used belong to three broad families: porphyrins, ruthenium complexes and pyrene derivatives. These molecules are excited in ultraviolet (pyrene) or in visible wavelengths (ruthenium). Some (porphyrins) can be excited over a large spectrum covering the ultraviolet and visible. Emission occurs in the visible portion of the spectrum.

The sensitivity to oxygen, more commonly called oxygen quenching, thus endows the molecule with sensitivity to air pressure, because the oxygen concentration is constant in the air. So, it is not a matter of sensitivity to pressure in the mechanical sense.

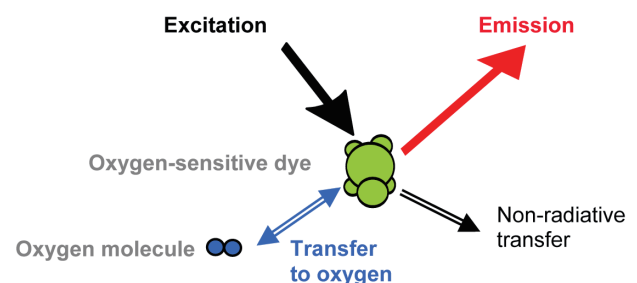


Figure 5 - Pressure sensitivity principle.

Composition of a PSP coating

In practice, the application of paint on the model requires two different layers. The model is first coated with a screen layer, which hides the luminescence of the model and increases the emission intensity by reflecting both the incident excitation radiation and the PSP emission. Then the active layer consists of a porous binder mixed with the luminescent molecule. The binder must be porous because the PSP principle is based on transfers with oxygen molecules. Only if the binder is porous enough will the oxygen partial pressure in the paint be equal to that in the flow. The PSP response time depends on the paint porosity and thickness and is usually about one second. The thickness of the paint is in the range 30–50 μm . PSP coatings are applied with a spray gun.

Intensity measurement method

The intensity method considers the luminescence emitted under a continuous illumination. Another method considers that the rate of luminescence decreases after a brief excitation (see box 2). It can be shown that the sensitivity obeys the Stern–Volmer law over a large range. This law is:

$$\frac{I_{ref}}{I} = A_{pref} + B_{pref} \frac{p}{p_{ref}} \quad (4)$$

Box 2- Lifetime method

If a PSP molecule is excited briefly, it can be shown that its response is:

$$I(t) = I_{t=0} e^{-t/\tau} \quad (\text{i})$$

where τ is the radiance lifetime. It can be shown that τ is expressed in the form:

$$\frac{\tau}{\tau_0} = 1 + \alpha p \quad (\text{ii})$$

where τ_0 is the lifetime without oxygen. The lifetime varies considerably from one dye to another. It is of the order of 100 ns for pyrene-based paints and of the order of 100 μ s for porphyrin-base paints.

The response under continuous excitation is found by integrating Eq. (i):

$$I = I_{t=0} \int_0^{t \rightarrow \infty} e^{-\eta/\tau} d\eta = I_{t=0} \tau \quad (\text{iii})$$

$$\frac{I_{ref}}{I} = \frac{1 + \alpha p}{1 + \alpha p_{ref}} = \frac{1}{1 + \alpha p_{ref}} + \frac{p}{1 + \alpha p_{ref}} \frac{p}{p_{ref}} \quad (\text{iv})$$

According to the Stern–Volmer equation (4), the values of coefficients A and B are:

$$A = \frac{1}{1 + \alpha p_{ref}}, \quad B = \frac{p_{ref}}{1 + \alpha p_{ref}} \quad (\text{v})$$

So there is a strict equivalency between the Stern–Volmer law and the radiance lifetime law.

In this equation, the subscript *ref* indicates a reference value, generally taken at atmospheric pressure. I_{ref} is the intensity emitted under continuous excitation at the reference pressure p_{ref} , while I is the intensity emitted at the pressure p .

Constant A_{pref} gives the ratio of the intensities between the reference pressure (usually atmospheric) and the value at vacuum (i.e., with no oxygen). Since the oxygen captures a part of the excitation energy, the emission intensity decreases with an increasing partial pressure of oxygen, i.e., as the pressure rises

As I/I_{ref} is equal to one at the reference pressure, the sum $A_{pref} + B_{pref}$ is also equal to one and therefore B_{pref} is always less than one. However, Eq. (4) is only approximate because it does not take many effects into account – especially that of temperature. Polynomials of the following form are therefore used in practice:

$$\frac{I_{ref}}{I}(T, p) = \sum_{i=0}^n A_i T^i + \sum_{i=0}^n \sum_{j=1}^m B_{ij} T^i \frac{p^j}{p_{ref}} \quad (5)$$

where the temperature T can have a large effect. Usual PSP temperature sensitivity is between 0.4 to 1%/K. For a sensitive PSP ($B \sim 1$), an uncontrolled 1K increase in the temperature produces a considerable error of 400 Pa to 1kPa around the ambient pressure.

Sources of errors

Temperature

The temperature is one of the main sources of error even for a low temperature sensitive PSP, like pyrene-based paints which have a temperature sensitivity of 0.4% / K leading to an error in pressure of 500 Pa for 1 K. The temperature difference between the reference (or wind-off) image, which is taken when there is no flow in the wind tunnel, and the wind-on image, taken under the flow, must be taken

into account as well as the temperature gradient on the model surface under the aerodynamic flow.

Temperature measurements taken using a few temperature sensors are limited to uniform variation of temperature, which is never the case. Such sensors can be useful for the reference image when thermal equilibrium is reached.

We can assess the temperature map for the wind-on images by calculating the recovery temperature. Since this temperature depends on the local Mach number, the calculation is then an iterative method. Another possibility is to measure the temperature map with an infrared camera. This solution can be difficult to install in wind tunnel test sections because special infrared optics are required (see § Example of applications).

Binary paints can also be used to correct for the temperature variation. The principle is to add a second dye in the PSP (see box 3). This dye must be insensitive to pressure and, if it has the same temperature sensitivity as the pressure dye, the ratio between the two emissions will be insensitive to temperature. The measurements are also corrected for the intensity variations. This is the ideal case.

The second dye can be used as a temperature sensor, like in TSP (Temperature Sensitive Paint) where the emission spectra exhibits two different wavelength ranges with different temperature sensitivities. In this case, three images are required: one for the pressure, one the temperature and one for the intensity variations.

Intensity variation

Each uncontrolled variation in intensity will lead to a pressure uncertainty in the final results. Variations in intensity measured by the camera can be due to an unstable excitation source or to a model movement and/or deformation between the reference image and the wind-on image.

Source stability can be checked on a sequence of images. Continuous stable sources provide stability better than 0.1% (rms value) on a sequence of 20 images which are needed to reduce the camera shot noise (see § Instrumentation). The sequence duration is about 5 minutes and is representative of wind tunnel test acquisition conditions. Model displacement between wind-off and wind-on images under aerodynamic loads and model deformation leads to a change of illumination field on the surface. Binary paint (see box 3) can be used to correct for these effects provided that the two set of images are properly aligned before processing, taking the 3D model geometry into account. Dedicated software called AFIX_2 has been developed at Onera to process the images [15] (one of its main tasks is to calibrate the camera, see box 5).

Instrumentation

PSPs can be excited by ultraviolet or visible spectrum light, depending on the dye used. Onera's paint contains a pyrene derivative as the pressure sensor and a rare earth oxysulfide as the reference component, which require UV light as excitation. We use a continuous Mercury-Xenon lamp which is extremely powerful (100 times standard Hg lamp) and very stable.

The PSP technique is a photometry technique and therefore the camera used for intensity measurements has to satisfy specific require-

ments. Scientific grade CCD cameras are cooled in order to reduce the dark current. They have a quantum efficiency up to 90 % in the visible range and a high full well capacity (300,000 electrons) which provides high sensitivity and dynamics (16 bits). Note that photon shot noise is a fundamental property of the quantum nature of light. As a consequence, photon shot noise is unavoidable and always present in imaging systems. Image averaging is the only way to reduce its effect.

In the case of binary paints that include a reference dye, there are two images so two filters are needed and three for the TSP/PSP application. A filter holder can be used to change the filter in front of the camera, but then the two images are no longer synchronous. This means that the excitation intensity should not change between the two images, requiring a source stability better than 0.1 %.

Some additional corrections can be achieved like the camera linearity and the flat field defects. The flat field correction is made to compensate for the non-uniformity of the CCD response. A flat field image is usually obtained by imaging a uniform field of view. Since it is nearly impossible to create a uniform scene, dedicated devices are used as integrating spheres. However, vignetting created by the lens is often larger than the non uniformity of the CCD. Therefore the lens must be calibrated too. This is a tedious task since vignetting depends on the aperture and on the focus distance.

Box 3 - Binary paint and TSP principle

PSPs that use a second dye are called binary paints. The second dye, used as reference to correct for variation of illumination, should be insensitive to the pressure and its emission spectrum must be clearly distinguishable from that of the pressure-sensitive dye (Figure B3 - 01).

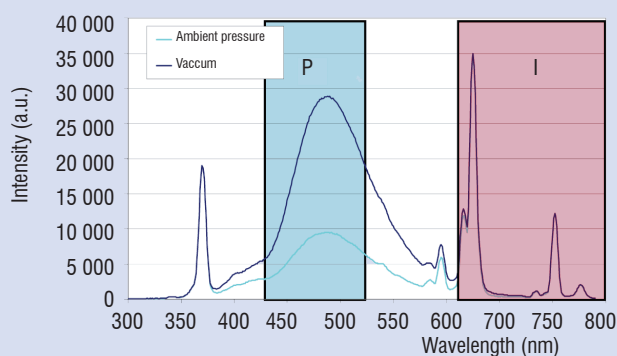


Figure B3 - 01 - Emission spectra of the Onera's PSP binary paint showing the pressure sensitivity (P filter) and the reference measurement (I filter).

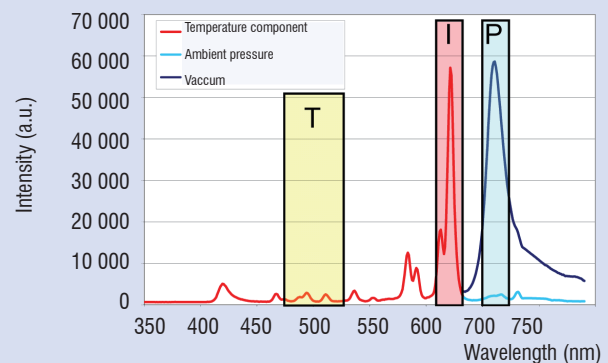


Figure B3 - 02 - Emission spectra of a PSP/TSP binary paint showing the pressure sensitivity (P filter), the temperature measurement (T filter) and the reference measurement (I filter).

The image corresponding to the reference dye can then be selected out by a filter. This view is often called the intensity image. The pressure image provided by the pressure sensitive dye is then divided by the intensity image, which compensates for the intensity fluctuations. The main drawback of the binary paint strategy is that two images are required: this means using two cameras or a single camera equipped with a filter holder.

An extension of the binary paint concept is using the second component as a temperature sensor, thus combining the PSP and TSP (Temperature Sensitive Paint) measurement techniques (Figure B3 - 02). In this case three images are required. The temperature image is used in the calibration law (eq. 5) to correct pressure measurements.

Box 4 - Pressure Sensitive Paint: uncertainty

The pyrene-based paint developed at Onera has a pressure sensitivity of 80%/100 kPa and a temperature sensitivity of 0.4%/K. Thus the uncertainty on pressure due to a temperature variation of 1 K is 500 Pa.

Similarly, any variation in intensity due to the source stability or to the model's movement of 0.1% represents an uncertainty of 100 Pa (50 Pa rms). PSP is an absolute measurement technique, so this value corresponds to a more important uncertainty on the C_p coefficient which is a relative pressure parameter under low speed flow where pressure variations are small ($\Delta C_p=0.04$) than under transonic flow conditions ($\Delta C_p=0.01$).

Example of applications

PSP was initially developed for transonic applications where the demand was greatest. Since low speed tests play an important role for the design phase of aircraft, PSP technology has also been developed for small pressure variations in the pressure range between 80 and 100 kPa. A great deal of effort has been put into controlling all of the sources of errors which limit the accuracy of the technique [16, 17, 18].

We present a test performed in a low speed wind tunnel located at Onera Lille center with wind speed at 40 m/s. The test item was a fighter aircraft and the PSP was applied on the right wing, both on the pressure side and on the suction side. The model was equipped with canards located upstream of the wings. The canards have a strong effect on the wing and the aim of the test was to understand the decrease in efficiency on the trailing edge flap at high angle of attack (figure 6).

Simultaneously, temperature measurements were taken using an infrared camera with 70 mK of resolution. The temperature maps obtained on the suction side are uniform with a temperature variation of 0.2 K. On the pressure side, the IR images show a pattern which represents the structure of the model (figure 7). The main part of the wing is made of steel while the other part is filled with a resin. The temperature variation on the surface remains low (0.7 K) however temperature correction needs to be done on the pressure images. If not, the PSP images will show the same pattern as the temperature image and, in this case, we have checked that the discrepancy in pressure represents 300 Pa.

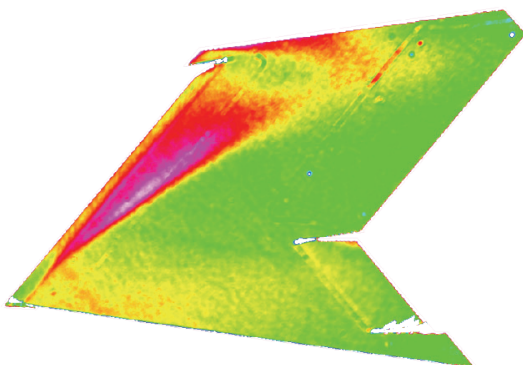


Figure 6 - PSP image on the wing suction side at 18° of angle of attack. The canard effect is visible near the wing fuselage junction.

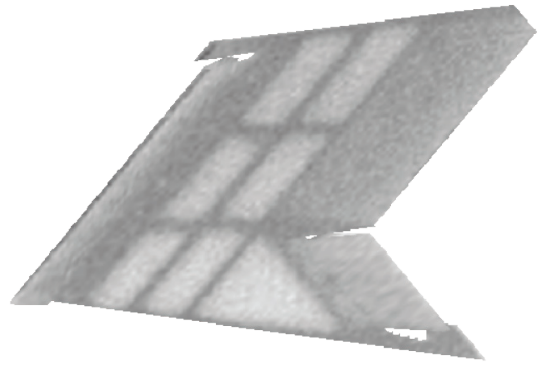
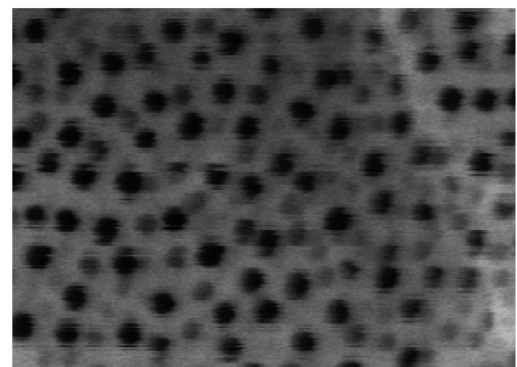


Figure 7 - Infrared image on the pressure side. $\Delta T_{\max}=0.7K$.

Unsteady PSP measurements

Application to unsteady pressure measurements is a new challenge for the PSP technique as it requires a fast responding coating [19]. Highly gas diffusive materials are needed as a binder for the unsteady PSP because the response time of the PSP depends on the gas diffusivity in the binder. One solution is to remove the binder and to use a fast responding PSP based on porous anodized aluminum with the dye adsorbed on the surface (AA-PSP) [20, 21, 22]. This type of coating (figure 8) gives a quite short response time of the order of 100 μs . AA-PSP has been used in a blow down supersonic wind tunnel to investigate the flow field topology inside a nozzle during the transient phase and to assess the pressure gradient at the outlet region during the steady state phase (figure 9). Images are acquired by using a fast frame rate camera equipped with a CMOS sensor, 12 bits dynamic range, at a rate up to 5,000 images per seconds (figure 10).



200 nm



Figure 8 - Self organized formation of hexagonal pores on the Anodized-Aluminum surface (scanning electron microscopy)

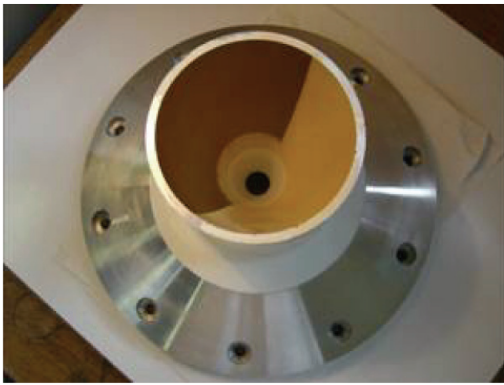


Figure 9 - Nozzle model with AA-PSP on half part of the inner surface

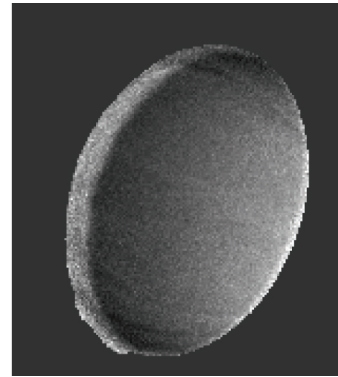


Figure 10 - Pressure image obtained during the transient phase.

Video - <http://www.aerospacelab-journal.org/al1/Surface-mapping-methods>

Box 5 - Camera calibration

Imaging methods address this question: where is the object in the image? The answer for the earliest mapping methods, such as infrared thermography, was very simple: the camera axes were aligned with the object axes. Assuming that this one was planar, which was often the case, a linear relation was established between the image and the object. This approach is still valid for some methods, such as 2C PIV. However, most of the applications have to deal with 3D objects and/or with a 3D camera arrangement. So the original question becomes: where is the camera in relation to the object? This problem is known as the pose problem [26] and is well known by the Computer Vision (CV) community. It was solved very early (Grüner, 1841!) and requires at least four known imaged points. Six parameters are identified which are three rotations and three translations. They are called the external parameters. The image is then created using the pinhole model (Figure B5 - 01).

However, using only the external parameters is not sufficient: the focal length must be known. You might think that the focal length number provided with the lens system could be used, but... this is only a rough estimate! Every photographer knows that changing the focus distance changes the viewed size of the object slightly, which means that the focal length depends on the focus distance! As a consequence it is also a parameter and is called an internal parameter since it only depends on the lens, not on the camera's location. But this is only the beginning of the story: adjusting the external parameters and the focal length is done with a minimization criteria and the final standard deviation is often greater than 1 pixel, which is really too much for a lot of quantitative methods. Then extra parameters were added: the first ones were the pixel ratio and the skew factor, which models the possible rhomboid shape of the camera sensor. These two parameters were firstly identified by CV because they can be determined with analytical methods [27]. But the real world is more complex and in practice these two parameters are negligible in relation to other parameters that model lens distortions. All of these parameters along with the focal length are grouped together in the internal parameter set.

The first one is the radial distortion parameter K_1 , which creates a symmetric cushion effect. Then comes the lateral distortion, modeled with two parameters called P_1 and P_2 . The equations that give the lens distortion are:

$$x_d = x + x r^2 K_1 + P_1 (r^2 + 2x^2) + 2 P_2 x z \quad y_d = y + y r^2 K_1 + P_2 (r^2 + 2y^2) + 2 P_1 x z$$

where x, y are the image coordinates and x_d, y_d are the corrected coordinates. Note that the lens distortions could be modeled with two polynomial of the third order, which would introduces 20 parameters, which is much more than the 3 lens deformations parameters! Figure B5 - 02 shows the (exaggerated) effect of these parameters. In practice, at least two other parameters are used which are the coordinates of the lens axis in the image plane. It can usually be assumed to be exactly at the center of the image, but this may be not true for some cameras or for 3C PIV measurements that use a Sheimpflug device.

Calibration is done with a calibration body that is a flat plate covered with markers, as shown in Figure B5 - 02. The white ones are used for an automatic alignment and then the calibration is fully automatic. Several images are used. The calibration plate must be moved in the measurement volume and must be turned so that the upper left corner becomes the lower right corner. The reason is that the calibration body always suffers from small defects. Changing the plate orientation compensates for them. However, it has been demonstrated that no compensation can be made some defects, such as a twist. The marker locations then have to be adjusted, which is known in CV as "bundle" adjustment.

The uncertainty can be as low as 0.06 pixels, which is the uncertainty of the marker detector. However, this is usually difficult to achieve because of blurring created by the out-of focus effect or by some small calibration body motion since this one is often moved manually. Usual values are closer to 0.4 pixels, while an uncertainty greater than 1 pixel means that something is going wrong.

Using all the latest tools, such as bundle adjustment, calibration is more a matter of know-how and skills than a scientific task, even if it can be deeply involved in scientific applications. However decreasing the uncertainty would require an advanced investigation into marker detection (the existing tool is already rather sophisticated) as well as modeling small sensor defects.

Visit the Onera web site www.onera.fr to learn more about calibration.

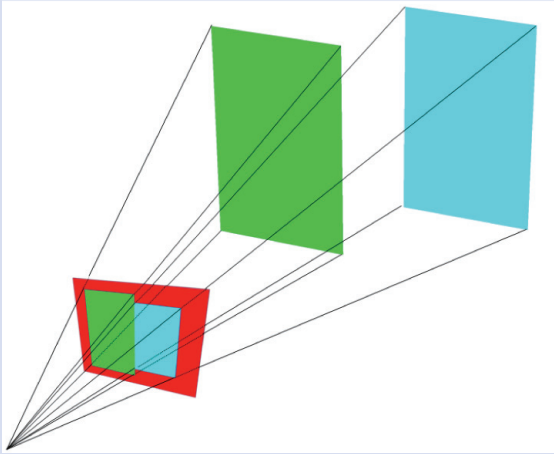


Figure B5 - 01 - The pinhole model.

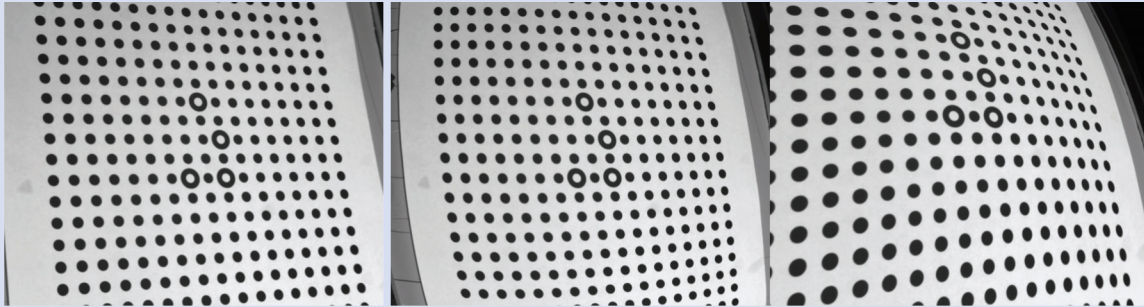


Figure B5 - 02 - The original image, enhanced cushion effect with K_1 , enhanced lateral distortion with P_1 and P_2 .

Model Deformation Measurement

Models used in wind tunnel testing are deformed by the aerodynamic loading. This may create a wing twist as large as 1° , while the acceptable uncertainty is lower than 0.1° ! As a consequence there are differences between the tested shape and the shape used for computations. As a matter of fact, for a long time these differences were thought to be caused by wind tunnel wall interference or by sting effects, while the real reason, wing deformation, was ignored. The likely reason is that the deformation level was unknown and barely measurable because of the lack of an appropriate method. Indeed, it is only recently [23] that model deformation has been considered to be a major source of errors that must be measured for every test.

There are several methods but the only one that provides real time results is based on marker detection and stereovision which is very well known by the Computer Vision (CV) community. Markers are stuck on the model surface which is imaged with two cameras. Figure 11 shows two typical images as well as a marker. The angle between the two cameras is close to 45° . These cameras (usually $2,000 \times 2,000$ pixels) must have been calibrated previously (Box 5). The challenge for applications in large facilities is the size of the calibration body. It has to be stiff but must not be too heavy and then cannot be expected without defects. This is why the calibration method includes a tool (known as bundle adjustment by CV), which is used to compensate for shape defects.

The basic tool for stereovision is marker detection. The final uncertainty depends on it, which is why a fast and accurate marker detector has been developed. Its uncertainty is of 0.06 pixels, which provides a measurement uncertainty lower than 0.1mm for a full scale of 1m. The twist uncertainty is lower than 0.05° , even at the wing tip.

The 3D location of the marker is obtained using the stereovision principle which is simple: a marker in an image defines a viewing line and the real point is located at the intersection of the two lines. However, they never intersect exactly and there is a small error which is called the epipolar error. The average epipolar error is a good indicator for camera calibration quality. It can be lower than 0.1 pixels and it is considered to be acceptable for values lower than 0.5 pixels. Larger values mean that the cameras start to become uncalibrated, because of the relative displacement relative to each other.

The Onera MDM system [24] is monitored by the wind tunnel control system as a usual measurement tool. It can work at a frequency of 10Hz and is mostly limited by the frame rate. Figure 12 is an example of bending measurement along a wing.

Up to now, this system could be compared to industrial vision systems and is more of an engineering application than a scientific one. However recent developments are scientific matters. The first development is related to the effect of thick windows (several centimeters) or a change of medium (air/pressurized air) that makes the standard pinhole model not completely reliable. A second one is tracking small parts of the wing and moving the cameras to track them when the model moves. The cameras would become uncalibrated (only the external parameters) and may be recalibrated to minimize the epipolar error [25]. A real scientific challenge would be to assess the effects of air density changes on the MDM measurements. These effects are created by the pressure changes, especially through the shock waves.

The MDM method can be used for other applications than wind tunnel testing. It can be used for conventional shape measurement, for flight testing or for scientific applications that require knowledge of an object's shape with a non contact method. This would be the case for PIV or LDV measurements close to the model's surface.

Box 6 - Model Deformation Measurement: uncertainty

The standard measurement uncertainty is 0.1mm for 1m, and twist uncertainty of 0.05°

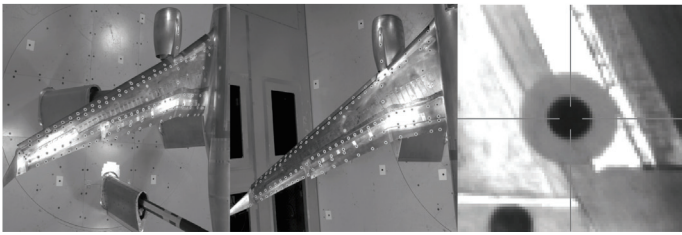


Figure 11 - The two images obtained by the two cameras and a marker.

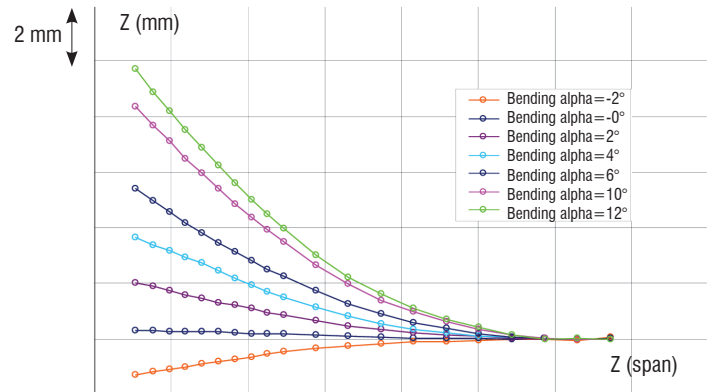


Figure 12 - A typical example of wing bending.

Wall Friction Measurement Using The Oil Droplet Technique

The drag of an airplane is due to pressure forces and friction forces, both contributions being nearly equal in cruise conditions. While surface pressure distribution is quite easy to measure, the direct measurement of wall friction is still a major challenge.

The friction force is generally determined indirectly, i.e. either from velocity measurements above the surface with an assumption for the velocity distribution or from analogies between friction and heat transfer. There are however several methods for directly determining the wall friction, some having been known for a long time, such as the use of surface balances or the oil film technique, and some being more recent, such as the use of micro-balances or flexible micro-cylinders.

The oil film technique [28] is based upon the analysis of the law governing the spreading of a very thin film of viscous fluid under the action of the wall friction. In the simple case of a uniform wall friction, except close to the ends where capillarity effects are important, the film grows linearly in space. Moreover, the film gets thinner as time increases and it spreads. The film height h is thus given by the relation

$$h(x, t) = \frac{\mu_0 x}{\tau_w t} \quad (6)$$

where μ_0 is the oil viscosity, τ_w the wall friction, x the abscissa and t the time. The film thickness can be determined by an interferometric technique. When the film is illuminated by a monochromatic light, fringes can be observed, which can be related to the changes

in the film thickness, as shown in figure 13. This figure also shows the spreading of the film and changes in film thickness leading to changes in the fringe spacing.

When the wall friction is not constant, the expression of the film thickness is very tricky, so that the determination of the friction from the film thickness is far from simple and accurate. Moreover, the film thickness can also increase or decrease longitudinally, which cannot be determined by the fringe pattern which only gives information about a change in thickness, not its sign.

Firstly, Onera [29] proposed the use of at least two illumination wavelengths, so that the comparison of the information given by the fringe patterns for the various wavelengths gives the sign of variation of the film thickness. Another strategy developed at Onera is to use only very little droplets, a few square millimeters in surface, so that the wall friction can be assumed constant. Moreover, an analysis of the interfringe process has given deep insight in the optical properties of the material the oil droplet has to be deposited on [30]; small Mylar stamps are good candidate. This analysis also shows that the method can work looking at the fringes from under a glass surface. Onera has applied this technique from low speed to transonic and supersonic speeds. Figures 14 and 15 provide examples of measurements, taken in the WALLTURB European project, respectively for a nearly zero pressure gradient flow and for a severe positive pressure gradient flow. The measured skin friction is compared with micro-PIV results and with indirect determination from the Clauser plot. This approach is shown to be reliable and able to measure very low friction levels [30].

This technique can be used on any model, without special equipment, provided an optical access is possible.

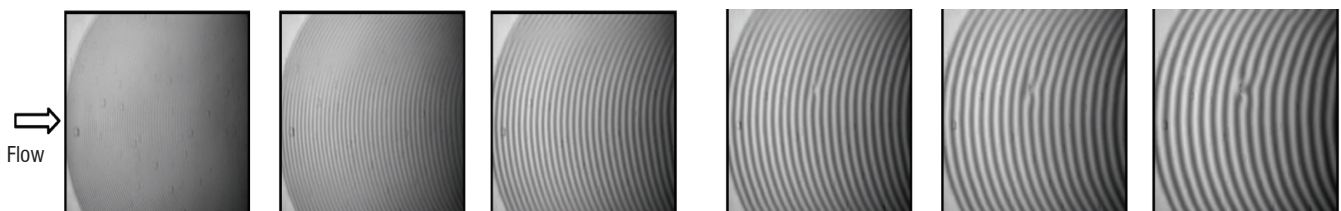


Figure 13 - Changes in the fringe pattern on the oil droplet with time.

Conclusion

The methods presented here are quite mature and are used routinely in wind tunnel testing. However significant progress has been made recently concerning the “details”. For example, an accurate calibration of the camera used for PSP has significantly decreased the uncertainty of PSP. Uncertainty is the keyword: this is the right guide to selecting the required developments. From this point of view, maybe the most important recent progress is this rigorous assessment of uncertainty that has nothing in common with the old rules of thumb. The research into PSP concerns its application for unsteady measurements, for which there are many requests. In the case of two other

methods, *IrT* and MDM, the aims are quite similar: to reach the limits, which is a 3D data reduction for *IrT* and measuring small details for MDM. This would be the final step and highlights the lack of a full mapping measurement method for shear stress. This measurement is often considered to be as important as pressure, but there is still no practical method for large wind tunnels. There are some solutions, such as the oil droplet method presented in this article, but none of them are as developed as PSP, for example. This, then, is a major scientific challenge and we can expect to see more and more effort put into it in future ■

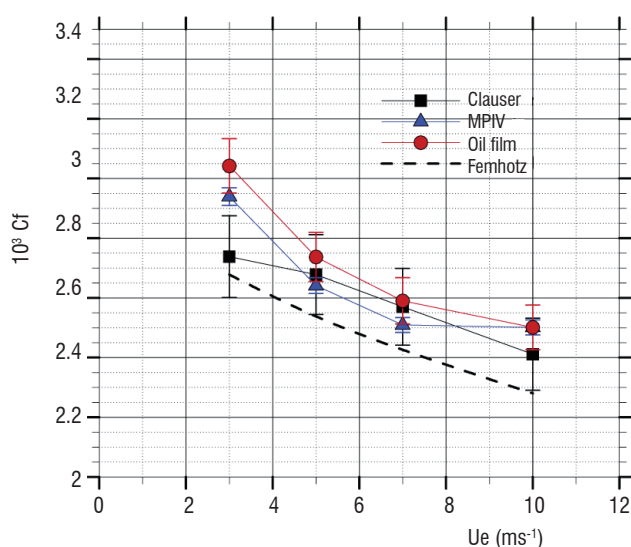


Figure 14 - Skin friction coefficient determination for nearly zero pressure gradient flow.

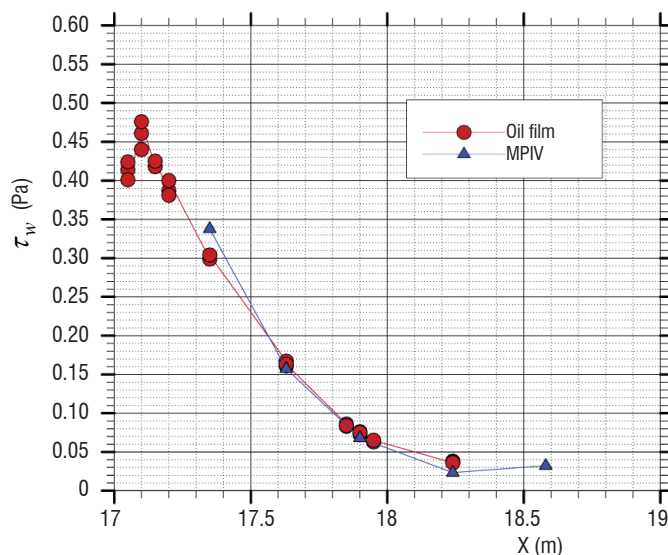


Figure 15 - Wall shear stress measurements for a strong adverse pressure gradient boundary layer.

References

- [1] U. FEY - *Transition Detection by temperature Sensitive Paint at Cryogenic Temperatures in The European Transonic Windtunnel (ETW)*. 20th International Congress on Instrumentation in Aerospace Simulation Facilities, ICIAF 2003 Record, Göttingen, Germany, August 25 –29 , pp. 77 – 88, 2003.
- [2] H.S. CARSLAW, J.C. JAEGER - *Conduction of Heat in Solids*. Oxford University Press, New-York, 1959.
- [3] D.L. SHULTZ, T.V. JONES - *Heat Transfer Measurements in Short Duration Hypersonic Facilities*. AGARDograph 168, 1973.
- [4] L. DE LUCA, G. M. CARLOMAGN, G. BURESTI - *Boundary Layer Diagnostics by Means of An Infrared Scanning Radiometer*. Experiments in fluids 1990, vol. 9, n° 3, pp. 121-128.
- [5] Y. LE SANT, M. MARCHAND, P. MILLAN AND J. FONTAINE - *An Overview of Infrared Thermography Techniques Used in Large Wind Tunnels*. Aerospace Science and Technology, Vol. 6 Issue 5. Pages 355-366, September 2002.
- [6] J. V. BECK, B. BLACKWELL, C. ST CLAIR - *Inverse Heat Conduction: Ill Posed Problems*, Wiley Interscience, New York, 1985.
- [7] D. NORTHAUSER, P. MILLAN - *Resolution of Three-Dimensional Unsteady Inverse Problem by Sequential Method Using Parameter Reduction and Infrared Thermography Measurements*. Numerical Heat Transfer, Part. A, vol. 37, pp. 587-611, 2000.
- [8] A. HOORNAERT, C. PELISSIER, Y. LE SANT, F. THIVET, P. MILLAN - *Rear Infrared Thermography in Heat Fluxes Determination on Hypersonic Vehicles*. 7th International Conference on Quantitative Infrared Thermography, QIRT 2004, von Karman Institute for Fluid Dynamics, 5-8 July 2004, Rhode-St-Genèse, Belgium
- [9] T. LIU, J.P. SULLIVAN - *Pressure and Temperature Sensitive Paints*. Springer-Verlag, 2004.
- [10] Y. LE SANT, M.-C. MÉRÉENNE - *Surface Pressure Measurements by using Pressure-Sensitive Paints*. Aerospace Science and Technology, 9, 2005, pp. 285-299.
- [11] Y. MEBARKI - *Pressure Sensitive Paints: from Laboratory to Wind Tunnel*, 22nd ICAS congress, Harrogate, England, 2000.
- [12] J.H. BELL, E.T. SHAIRER, L.A. HAND, R.D. MEHTA - *Surface Pressure Measurements Using Luminescent Coatings*, in: *Annual Review of Fluid Mechanics*, Vol. 33, March 2001, pp. 155–206.
- [13] C. KLEIN, R.H. ENGLER, U. HENNE, W. SACHS - *Application of Pressure Sensitive Paint for Determination of the Pressure Field and Calculation of the Forces and Moments of Models in Wind Tunnel*. Experiments in Fluids, 2005, Vol. 39, pp475-483.
- [14] Y. MEBARKI, *Peintures Sensibles à la Pression: Application en Soufflerie Aérodynamique*. Thesis presented at Lille 1 University, 1998.
- [15] Y. LE SANT, A. DURAND, M.-C. MERIENNE - *Image Processing Tools Used for PSP and Model Deformation Measurements*. 35th AIAA Fluid Dynamics Conference and Exhibit, Toronto, Paper AIAA 2005-5007.
- [16] R. ENGLER, M.-C. MERIENNE, K. KLEIN, Y. LE SANT - *Application of PSP in Low Speed Flows*. Aerospace Science and Technology, Vol. 6, N° 5, 2002.

- [17] J. H. BELL - *Applications of Pressure Sensitive Paint to Testing at Very Low Speeds*. 42nd AIAA Aerospace Sciences Meeting and Exhibit, Reno, Nevada, Paper AIAA 2004-0878.
- [18] M.C. MERIENNE, Y. LE SANT - *Reliable PSP Application and Data Processing at Low Speed Flow Conditions*. 24th AIAA Aerodynamic Measurement Technology and Ground Testing Conference, San Francisco, Paper AIAA 2006-3632.
- [19] C. KLEIN, U. HENNE, W. SACHS, R.H. ENGLER, Y. EGAMI, V. ONDRUS, U. BEIFUSS, H. MAI - *Application of Pressure-Sensitive Paint for Determination of Dynamic Surface Pressures on a Rotating 65° Delta wing and an oscillating 2D profile in transonic flow*. ICASF, Pacific Grove, 2007.
- [20] H. SAKAUE, K. ASAI, J.P. SULLIVAN, Y. IJIMA, T. KUNIMASU - *Anodized aluminum Pressure Sensitive Paint in a Cryogenic Wind Tunnel*. 45th Int. Instrumentation Symposium, Instrument Society of America, Albuquerque, NM, 1999.
- [21] M. KAMEDA, T. TABELI, K. NAKAKITA, H. SAKAUE, K. ASAI - *Image Measurements of Unsteady Pressure Fluctuation by a Pressure-Sensitive Coating on Porous Anodized Aluminum*. Measurement Science and Technology, Vol. 16, 2005, pp. 2517-2524.
- [22] M.C. MERIENNE, D. COPONET, J.M. LUYSSSEN. - *Unsteady Pressure Field Investigation in a Nozzle by Using Anodized-Aluminum PSP Technique Under Supersonic Flow Conditions*. 26th AIAA Aerodynamic Measurement Technology and Ground Testing Conference, Seattle, Paper AIAA 2008-3946.
- [23] T. LIU, R. RADEZTSKY, S. GARG, L. CATTAFESTA - *A Videogrammetric Model Deformation System and its Integration with Pressure Paint*. 37th AIAA Aerospace Sciences Meeting and Exhibit, AIAA 99-0568, January 11-14, 1999, Reno, NV.
- [24] Y. LE SANT, A. MIGNOSI, G. TOURON, B. DELÉGLISE, G. BOURGUIGNON - *Model Deformation Measurement (MDM) at Onera*. 25th AIAA Applied Aerodynamics Conference, paper 2007-3817, Miami, FL, 25-28 June 2007.
- [25] R. HARTLEY, A. ZISSERMAN - *Multiple View Geometry in Computer Vision*. Cambridge University Press, 2000.
- [26] R. HARALICK, C.N. LEE, K. OTTENBERG, M. NÖLLE - *Review and Analysis of Solutions of the Three Points Perspective Pose Estimation Problem*. International Journal of Computer Vision, vol. 13, n°3, pp 331-356, 1994.
- [27] R.Y. Tsai - *An Efficient and Accurate Camera Calibration Technique for 3D Machine Vision*. Proceedings of IEEE Conference on Computer Vision and Pattern Recognition, Miami Beach, FL, USA, 1986, pp. 364-374.
- [28] L. H. TANNER, L. G. BLOWS - *A Study of the Motion of Oil Films on Surfaces in Air Flow, With Application to the Measurement of Skin-Friction*. Journal of Physics E, vol. 9, N° 3, 1976.
- [29] J. M. DESSE - *Oil-Film Interferometry Skin-Friction Measurement Under White Light*. AIAA Journal, Vol. 41, N° 12, pp. 268-2477, December 2003.
- [30] G. PAILHAS, P. BARRICAU, Y. TOUVET, L. PERRET - *Friction Measurement in Zero and Adverse Pressure Gradient Boundary Layer Using Oil Film Interferometric Method*. Experiments in Fluids Volume 47, Issue 2 (2009), 195-207. (ONERA TPNP 2009-141).

Acronyms

PSP (Pressure Sensitive Paint)
MDM (Model Deformation Measurement)
CARS (Coherent Antistokes Raman Spectroscopy)
IrT (Infrared Thermography)
TSP (Temperature Sensitive Paint)
AA-PSP (Anodized Aluminum - PSP)

AUTHORS



Yves Le Sant Researcher at Onera since 1983. His first studies concerned wall interferences and the development of an adaptive test section. Then he was involved in applying and developing many measurements methods, such as heat flux assessment, temperature and pressure sensitive paints and model deformation. His current activities are in the field of image processing applications, such as in Particle Image Velocimetry.



Bertrand Aupoix graduated from Supaero in 1976. He was awarded a PhD in 1979 and a "Thèse d'Etat" in 1987, both in the field of turbulence modeling. He is currently Research Director and head of the TMP, Turbulence, Modeling and Predictions, Research Unit at Onera Toulouse.



Philippe Barricau graduated in solid state physics from the «Institut National des Sciences Appliquées». Since 1998, he has worked in the field of instrumentation applied to aerodynamics. He has developed the optical arrangement of a Doppler Global Velocimetry system. He has also implemented the PIV technique in various Onera facilities and used the oil film technique to measure skin friction in various flows. Since 2008, he has been working on the development of sparkjet actuators for flow control applications.



Marie-Claire Mérienne joined Onera in 1980 as a technician in the composite materials department. She received her Engineering Diploma in Physical Measurements and Instrumentation from the Conservatoire National des Arts et Métiers, in 1989. Then, she joined the experimental Aerodynamics Department and, since 1994, she has been involved in the development of the PSP technique. Recently, a large part of her activity has been focused on unsteady applications.



Guy Pailhas, a research engineer at Onera is in charge of experimental studies in the Turbulence Modeling and Prediction Unit. A large part of his activity is devoted to the analysis of the structure of turbulent shear flows. Recently, he focused his efforts on skin friction measurement in complex flows by means of the interferometric oil film technique.



Yann Touvet, graduated from the Institut Universitaire de Technologie in Toulouse. He is currently working as a technician at the Turbulence Modeling and Prediction Unit of the Aerodynamics and Energetics Modeling Department at Onera Toulouse.



Philippe Reulet, Dipl. Ing. Dr., responsible of Aerothermics activity in C2A Research Unit, graduated in 1992 from the «Ecole Centrale Paris». In 1997, he received his Ph.D. in Fluid Mechanics and Energetics from «Ecole Nationale Supérieure de l'Aéronautique et de l'Espace». Since 1998, he has been working at Onera in the field of experimental and numerical thermal analysis.